Exclusive W^+W^- production measured with the CMS experiment and constraints on Anomalous Quartic Gauge Couplings

Manfred Jeitler[*][†]

Institute of High Energy Physics of the Austrian Academy of Sciences, Vienna, Austria
E-mail: manfred.jeitler@cern.ch

A search for exclusive or quasi-exclusive W^+W^- production induced by photon-photon exchange in pp collisions at $\sqrt{s} = 8$ TeV is reported using data corresponding to an integrated luminosity of 19.7 fb^{-1}. Events are selected by requiring the presence of an electron-muon pair with large transverse momentum $p_T > 30$ GeV and no associated charged particles detected from the same vertex. The observed yields and kinematic distributions are compatible with the Standard Model prediction for exclusive and quasi-exclusive W^+W^- production. The dilepton transverse momentum spectrum is studied for deviations from the Standard Model, and the resulting upper limits are compared to predictions assuming anomalous quartic gauge couplings.

---

[*]Speaker.

[†]For the CMS Collaboration.

1. Introduction

The LHC allows to investigate high-energy photon-photon interactions due to its high energy and luminosity. From the first data taken at a collision energy of $\sqrt{s} = 7$ TeV, measurements of $\gamma\gamma \to \mu^+\mu^-$ [1], $\gamma\gamma \to e^+e^-$ [2] and $\gamma\gamma \to W^+W^-$ [3] have been made in processes such as those illustrated in Fig. 1. The process $\gamma\gamma \to W^+W^-$ had never been observed before LHC. The signal topology investigated in this analysis is $pp \to p^{(*)}W^+W^-p^{(*)}$, where the $p^{(*)}$ indicates that in the final state the protons may either remain intact (production in an elastic collision) or can break up into other particles not seen by the CMS detector (proton dissociation).
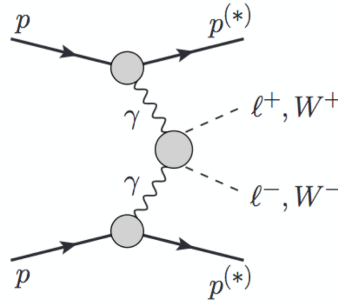

Figure 1: Production of lepton or W pairs by virtual photon exchange between protons.

The process $\gamma\gamma \to W^+W^-$ is allowed in the Standard Model (SM), where it can be mediated by genuinely quartic and by t- and u-channel diagrams as shown in Fig. 2.
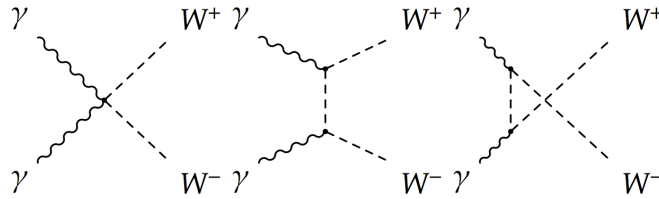

Figure 2: Quartic and t-channel diagrams contributing to the $\gamma\gamma \to W^+W^-$ process at leading order in the Standard Model.

At the same time, it is a promising process for searches of New Physics beyond the Standard Model (BSM). Possible deviations from the SM may be described by introducing genuine anomalous quartic gauge couplings (AQGC) parametrized by higher-dimension effective operators, which could arise in a number of different BSM scenarios. Before the LHC started taking data, such AQGCs in the quartic vertex $\gamma\gamma W^+W^-$ were constrained only by LEP data on tri-boson production and $WW \to \gamma\gamma$ scattering and by Tevatron measurements of $\gamma\gamma \to W^+W^-$ scattering. Ways to study AQGCs at the LHC complementary to the one described here are tri-boson production ($W\gamma\gamma$, $WW\gamma$, $WZ\gamma$), same-sign $WW \to WW$ scattering and decays with $Z + 2$ jets in the final state.

1.1 Signal and control channels

Cases where at least one of the W's decays hadronically would suffer from large QCD background and be difficult to distinguish from inclusive production. The decays $W^+W^- \to \mu^+\mu^-$ or

$W^+W^- \to e^+e^-$ would be dominated by Drell-Yan events and by $\gamma\gamma \to \ell^+\ell^-$ production. Therefore, the final state selected for the signal in this analysis is $W^+W^- \to \mu^{\pm}e^{\mp}$ (with undetected neutrinos). This signature also contains $W^+W^- \to \tau^+\tau^-$ signal events as well as Drell-Yan and $\gamma\gamma \to \tau^+\tau^-$ background where one of the τ's decays into a muon and the other one into an electron. As opposed to exclusive production, inclusive W^+W^- production is always accompanied by soft particles from multiple parton interactions resulting in additional charged tracks. The experimental signal signature is therefore a muon-electron pair with high transverse momentum p_T (to suppress background), with both leptons coming from the same vertex and without any additional charged tracks in the detector.

Same-flavor leptonic events from $\gamma\gamma \to \mu^+\mu^-$ and $\gamma\gamma \to e^+e^-$ have been used as control samples to investigate the event selection efficiency in data as well as corrections from rescattering, i.e. additional hadronic activity due to strong-interaction effects between the protons.

1.2 The CMS detector

A detailed description of the CMS detector has been given elsewhere [4]. The most important parts of the detector for this analysis are the silicon tracker, which covers the region up to $|\eta| < 2.4$ in pseudorapidity, the electromagnetic crystal calorimeter and the muon system consisting of Drift Tubes, Cathode Strip Chambers and Resistive Plate Chambers. Silicon tracker and calorimeters are surrounded by a superconducting solenoid providing a strong magnetic field of 3.8 T resulting in an excellent momentum resolution ($< 1.5\%$ for muons of $p_T < 100$ GeV).

1.3 Modelling of anomalous quartic gauge couplings

The triple ($WW\gamma$) and quartic ($WW\gamma\gamma$) couplings contributing to the process investigated in this analysis as shown in Fig. 2 are related by gauge invariance in the SM. For quartic couplings, potential deviations from the SM have been quantified by introducing effective operators of dimension-6 [5] or of dimension-8 [6, 7, 8]. By including the additional constraint that the $WWZ\gamma$ vertex should vanish, a direct relationship between the numerical values of the parameters of these two formalisms can be established.

In both scenarios anomalous couplings would result in a rapid rise of the $\gamma\gamma \to WW$ cross section with energy and violate unitarity at scales below those reached in 8 TeV proton-proton collisions. This can be prevented by modifying the effective Langrangian and introducing a dipole form factor with a cutoff scale.

1.4 Data and Monte Carlo

The data used in this analysis are based on 19.7 fb^{-1} of proton-proton collisions collected by the LHC at a center-of-mass energy of $\sqrt{s} = 8$ TeV in 2012, at a mean pileup of 21 individual pp-collisions per bunch crossing.

The signal for both the SM and the AQGC contributions was simulated using MADGRAPH [9]. The samples for $\gamma\gamma \to \ell^+\ell^-$ both in elastic processes and with proton dissociation were produced using the LPAIR generator [10]. Inclusive backgrounds from diboson production, W+jets and $t\bar{t}$ were produced with MADGRAPH while inclusive Drell-Yan samples were simulated using

POWHEG [11]. The outgoing partons calculated by these programs were matched to parton showers from PYTHIA [12] and the results were passed through the GEANT4 [13] simulation of the detector.

2. Event selection

2.1 Signal channel

In the analysis leptons from the $\mu^\pm e^\mp$ final state of the signal as well as from the $\mu^+\mu^-$ and e^+e^- states of the control samples are required to have a transverse momentum of $p_T > 20$ GeV (with somewhat lower trigger thresholds) and to pass various optimized selection criteria. A threshold is also applied to the invariant mass of the dilepton system ($\ell^+\ell^- > 20$ GeV) to remove background caused by low-mass resonances for the $\mu^+\mu^-$ and e^+e^- final states.

The signal is then selected by vetoing events with any additional charged tracks (to remove background from inclusive diboson production) and by setting a threshold on the transverse momentum of the muon-electron pair ($p_T(\mu^\pm e^\mp) > 30$ GeV (to eliminate background from $\tau^+\tau^-$ production).

2.2 $\gamma\gamma \to \ell^+\ell^-$ control samples

The $\mu^+\mu^-$ and e^+e^- final states suffer from much higher background from direct $\gamma\gamma \to \ell^+\ell^-$ production and from Drell-Yan processes than the $\mu^\pm e^\mp$ channel and are therefore not used for the signal selection. However, they are very useful as control samples serving two purposes: first, they allow to investigate the efficiency loss due to the veto requirement on additional charged tracks; second, they allow to get a better handle on the proton-dissociation contribution to high-mass $\gamma\gamma$ interactions, which is not well known from theory.

2.2.1 Efficiency loss due to veto on extra tracks

In exclusive production, additional tracks may be misidentified as coming from the dilepton vertex although in fact they originate from other proton-proton collisions in the same bunch crossing (pileup). These are mostly forward tracks of low p_T, which are not modeled perfectly by the Monte-Carlo simulation. The loss of events due to such pileup tracks can be estimated by comparing a pure selection of elastic events to the simulation. To obtain such a pure selection we choose lepton pairs back-to-back in azimuth by requiring a small "acoplanarity": $|1 - \Delta\phi(\ell^+\ell^-)/\pi| < 0.01$, and with an invariant mass of the lepton pair far away from the Z peak ($m(\ell^+\ell^-) < 70$ GeV or $m(\ell^+\ell^-) > 106$ GeV). These requirements strongly suppress Drell-Yan and other inclusive backgrounds. These control samples show a marked deficit in the data compared to the simulation for both the muon and the electron channel (Fig. 3). By cutting even more on acoplanarity ($|1 - \Delta\phi(\ell^+\ell^-)/\pi| < 0.001$, i.e. selecting the leftmost bin in Fig. 3) one can further reduce the possible contamination from $\gamma\gamma \to \ell^+\ell^-$ where one or both of the protons dissociate. From this selection we determine a data-to-simulation ratio of 0.63 ± 0.04 for $\mu^+\mu^-$ and of 0.63 ± 0.07 for e^+e^-. This value is applied as an efficiency correction factor to the 0 extra tracks requirement for the $\gamma\gamma \to W^+W^-$ signal.

For exclusive production, mis-assigned tracks from other pileup vertices can only result in a loss of events. For inclusive background processes, pileup can also have the opposite effect
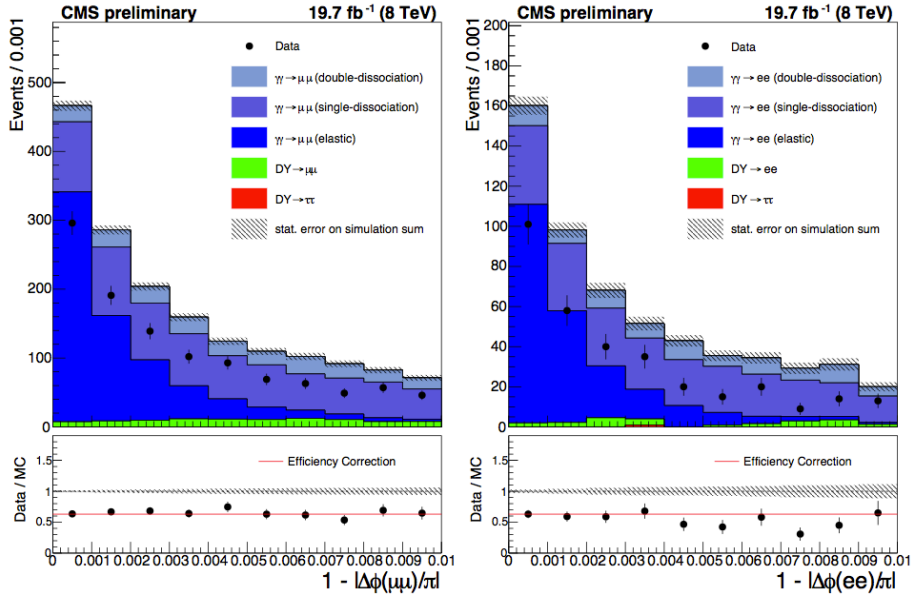
Figure 3: The acoplanarity for the $\mu^+\mu^-$ (left) and e^+e^- (right) final states in the elastic $\gamma\gamma \to \ell^+\ell^-$ control region with an invariant mass incompatible with $Z \to \ell^+\ell^-$ decays ($m(\ell^+\ell^-) < 70$ GeV or $m(\ell^+\ell^-) > 106$ GeV), with the requirement that there are no additional charged tracks. The red line shows the calculated correction to the 0 extra tracks efficiency.

when a track from the event itself (the "underlying event") is wrongly attributed to another vertex. For the largest background channel of inclusive W^+W^- production, it turns out that the net effect is zero and the simulation accurately reproduces the data, so that no correction is applied to the background.

2.2.2 Estimate of proton-dissociation contribution to high-mass $\gamma\gamma$ interactions

Simulations show that in high-mass $\gamma\gamma$ interactions one or both of the protons dissociate, which may result in events being rejected by the veto on extra tracks. To estimate this effect from data, a sample is selected where the dilepton invariant mass is greater than 160 GeV so that W^+W^- pairs can be produced on shell. The ratio of the observed number of events to the calculated number of elastic $pp \to p\ell^+\ell^-p$ events is used as a scale factor to calculate from the predicted elastic $pp \to pW^+W^-p$ events the total number of $pp \to p^*W^+W^-p^*$ to be expected when including proton dissociation. The numerical value of the scale factor thus obtained is F=4.10±0.43.

2.3 Backgrounds and systematics

The dominant background is di-boson production (mostly W^+W^- and some WZ events). It is strongly reduced by the veto on extra tracks from the $\mu^\pm e^\mp$ vertex. To confirm that the simulation models this background well a control region is chosen where the cut on the transverse momentum of the $\mu^\pm e^\mp$ pair is the same as for the signal ($p_T(\mu^\pm e^\mp) > 30$ GeV) but the veto on additional tracks is removed (1-6 extra tracks allowed; cf. Fig. 4). The data in this control region confirm the expectation from simulation (234.0 ± 7.8 (stat.) events expected and 214 events observed in data).

The MADGRAPH simulation for this background contribution in the signal region yields 2.0 ± 0.4 events (compatible with the PYTHIA result of 2.3 ± 0.8 events).
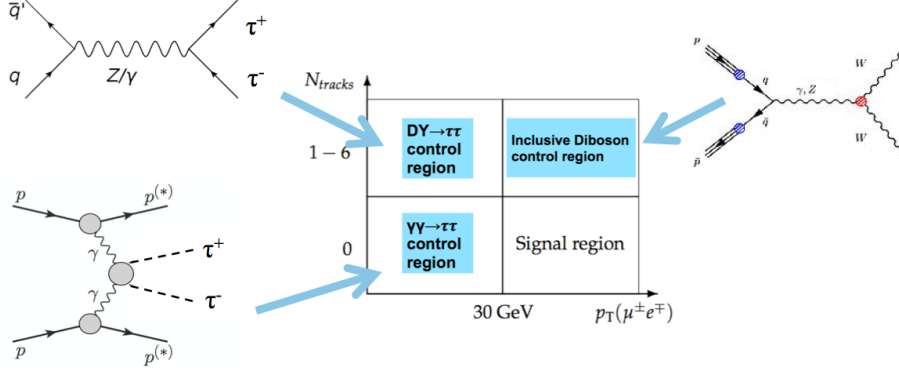

Figure 4: Control regions for verifying the simulation of three of the dominant background channels.

The background from Drell-Yan $\tau^+\tau^-$ production where one τ decays into a muon and the other into an electron (plus invisible neutrinos) is strongly suppressed by the veto on additional tracks. A control region at low transverse momentum ($p_T(\mu^\pm e^\mp) < 30$ GeV) and with the veto on extra tracks removed is dominated by Drell-Yan $\tau^+\tau^-$ events (cf. Fig. 4). There is some disagreement between these data and simulation at low μe invariant mass and low acoplanarity but at higher values of these variables (where inclusive WW production starts to dominate) the agreement is good. The simulation shows that no Drell-Yan $\tau^+\tau^-$ events survive in the signal region.

Background from $\gamma\gamma \to \tau^+\tau^-$ can also appear in exclusive events and can therefore not be completely suppressed by the veto on additional tracks from the dilepton vertex. It is, however, strongly reduced by the cuts on the transverse momentum of the lepton pair ($p_T(\mu^\pm e^\mp) > 30$ GeV) and of the individual leptons (20 GeV for both μ and e). A data control sample with the same veto on extra tracks as the signal but with inverted cut on transverse momentum $p_T(\mu^\pm e^\mp) < 30$ GeV) (cf. Fig. 4) confirms the simulation.

After including some less important background channels, the total expected background is 3.5 ± 0.5 (stat.) events, with the largest contribution coming from inclusive W^+W^- production while the expected SM signal is 5.3 ± 0.1 (stat.) events.

Systematic uncertainties are dominated by the proton dissociation probability (10.5%), where the leading contribution comes from the statistical error on data in the high-mass $\gamma\gamma \to \ell^+\ell^-$ control sample described in Section 2.2.2 (9.2%) and an additional effect of 5.0% is due to the uncertainties in the matrix elements used for simulation. The second most important systematic uncertainty comes from the estimate of the signal inefficiency introduced by the veto on extra tracks using the control samples of elastic-enriched $\gamma\gamma \to \ell^+\ell^-$ events and equals the statistical uncertainty in these samples. Minor contributions to the systematic uncertainty are due to the trigger and lepton identification efficiency (estimated from $Z \to \ell^+\ell^-$ events) and the measurement of the total luminosity.

3. Results

The signal region with the veto on extra tracks and the cut on the transverse momentum of $p_T(\mu^{\pm}e^{\mp}) > 30$ GeV contains 13 events while the expected background for this region is 3.5 ± 0.5 (stat.) events and the Standard Model predicts 5.3 ± 0.1 (stat.) events (Fig. 5). The distributions of $\mu^{\pm}e^{\mp}$ invariant mass, acoplanarity and missing transverse momentum are consistent with the SM plus background hypothesis. After correcting for experimental inefficiencies and extrapolating to full phase space, this corresponds to a cross section multiplied by the $\mu^{\pm}e^{\mp}$ branching fraction of $\sigma(pp \to p^*W^+W^-p^* \to p^*\mu^{\pm}e^{\mp}p^*) = 12.3^{+5.5}_{-4.4}$ fb compatible with the SM prediction of 6.9 ± 0.6 fb. The measurement excludes the background-only hypothesis by $3.6\,\sigma$.
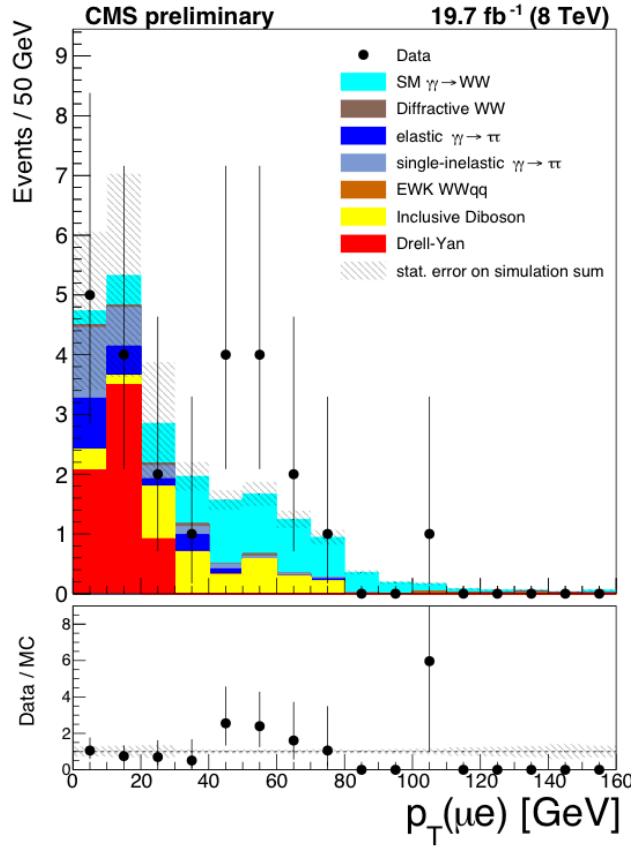

Figure 5: Muon-electron transverse momentum for events with zero associated tracks.

In terms of AQGC couplings, the data allow to obtain the following limits on the dimension-6 couplings defined in [5] when using a dipole form factor with $\Lambda_{cutoff} = 500$ GeV:

$$-1.1 \times 10^{-4} < a_0^W/\Lambda^2 < 1.0 \times 10^{-4} \text{ GeV}^{-2} \qquad (a_C^W/\Lambda^2 = 0)$$
$$-4.2 \times 10^{-4} < a_C^W/\Lambda^2 < 3.4 \times 10^{-4} \text{ GeV}^{-2} \qquad (a_0^W/\Lambda^2 = 0)$$

These values can be translated into the corresponding dimension-8 limits [6, 7, 8], which can be found in [14] together with more details of the analysis.

The two-dimensional limits in the a_0^W/Λ^2, a_C^W/Λ^2 space for this result and for the preceding CMS result from [3] are given in Fig. 6. The limits obtained in this analysis are based on the full 8-TeV data set and show a significant improvement over the first CMS analysis based on the initial 7-TeV data.
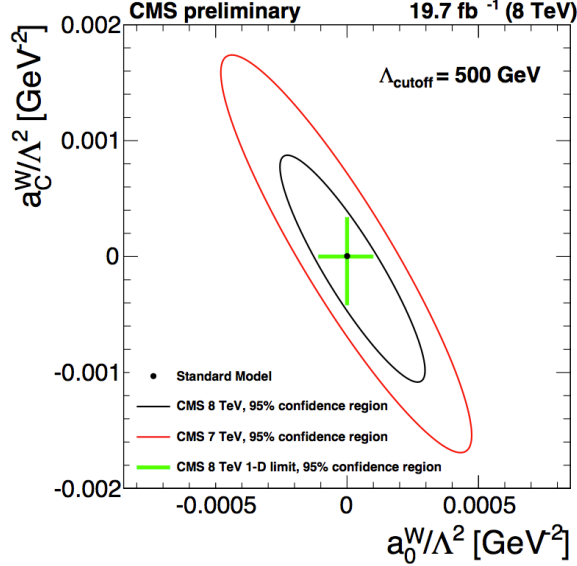

Figure 6: Excluded values of the anomalous coupling parameters a_0^W/Λ^2 and a_C^W/Λ^2 with $\Lambda_{cutoff} = 500$ GeV. The area outside the solid contour is excluded by this measurement at 95% CL. The predicted cross sections are rescaled to include the contribution from proton dissociation.

References

[1] CMS Collaboration, "Exclusive photon-photon production of muon pairs in proton-proton collisions at $\sqrt{s} = 7$ TeV", JHEP 01 (2012) 052, doi:10.1007/JHEP01(2012)052, arXiv:1111.5536.

[2] CMS Collaboration, "Search for exclusive or semi-exclusive photon pair production and observation of exclusive and semi-exclusive electron pair production in pp collisions at $\sqrt{s} = 7$ TeV", JHEP 11 (2012) 080, doi:10.1007/JHEP11(2012)080, arXiv:1209.1666.

[3] CMS Collaboration, "Study of exclusive two-photon production of W^+W^- in pp collisions at $\sqrt{s} = 7$ TeV and constraints on anomalous quartic gauge couplings", J. High Energy Phys. 07 (May, 2013) 116. 39 p.

[4] CMS Collaboration, "The CMS experiment at the CERN LHC", JINST 03 (2008) S08004.

[5] G. Belanger and F. Boudjema, "Probing quartic couplings of weak bosons through three vectors production at a 500-GeV NLC", Phys.Lett. B288 (1992) 201-209, doi:10.1016/0370-2693(92)91978-I.

[6] G. Belanger et al., "Bosonic quartic couplings at LEP-2", Eur.Phys.J. C13 (2000) 283-293, doi:10.1007/s100520000305, arXiv:hep-ph/9908254.

[7] O. Eboli, M. Gonzalez-Garcia, and J. Mizukoshi, "p p → j j e+- mu+- nu nu and j j e+- mu-+ nu nu at O(alpha(em)**6) and O(alpha(em)**4 alpha(s)**2) for the study of the quartic electroweak gauge

boson vertex at CERN LHC", Phys.Rev. D74 (2006) 073005, doi:10.1103/PhysRevD.74.073005, arXiv:hep-ph/0606118.

[8] M. Baak et al., "Working Group Report: Precision Study of Electroweak Interactions", arXiv:1310.6708.

[9] J. Alwall et al., "MadGraph 5 : Going Beyond", JHEP 06 (2011) 128, doi:10.1007/JHEP06(2011)128, arXiv:1106.0522.

[10] S. Baranov, O. Duenger, H. Shooshtari, and J. Vermaseren, "LPAIR: A generator for lepton pair production", in Hamburg 1991, Proceedings, Physics at HERA, vol. 3* 1478-1482. (see HIGH ENERGY PHYSICS INDEX 30 (1992) No. 12988). 1991.

[11] S. Alioli, P. Nason, C. Oleari, and E. Re, "A general framework for implementing NLO calculations in shower Monte Carlo programs: the POWHEG BOX", JHEP 06 (2010) 043, doi:10.1007/JHEP06(2010)043, arXiv:1002.2581.

[12] T. Sjostrand, S. Mrenna, and P. Z. Skands, "PYTHIA 6.4 Physics and Manual", JHEP 05 (2006) 026, doi:10.1088/1126-6708/2006/05/026, arXiv:hep-ph/0603175.

[13] GEANT4 Collaboration, "GEANT4: A simulation toolkit", Nucl.Instrum.Meth. A506 (2003) 250-303, doi:10.1016/S0168-9002(03)01368-8.

[14] CMS Physics Analysis Summary FSQ-13-008, available at http://cds.cern.ch/collection/CMS Physics Analysis Summaries